

# SelfText Beyond Polygon: Unconstrained Text Detection with Box Supervision and Dynamic Self-Training

WeiJia Wu<sup>1\*</sup>, Enze Xie<sup>2\*</sup>, Ruimao Zhang<sup>2</sup>, Wenhai Wang<sup>3</sup>, Guan Pang<sup>4</sup>, Zhen Li<sup>5</sup>,  
Hong Zhou<sup>1†</sup>, Ping Luo<sup>2</sup>

## Abstract

Although a polygon is a more accurate representation than an upright bounding box for text detection, the annotations of polygons are extremely expensive and challenging. Unlike existing works that employ fully-supervised training with polygon annotations, we propose a novel text detection system termed *SelfText Beyond Polygon (SBP)* with *Bounding Box Supervision (BBS)* and *Dynamic Self Training (DST)*, where training a polygon-based text detector with only a limited set of upright bounding box annotations.

For BBS, we firstly utilize the synthetic data with character-level annotations to train a *Skeleton Attention Segmentation Network (SASN)*. Then the box-level annotations are adopted to guide the generation of high-quality polygon-like pseudo labels, which can be used to train any detectors. In this way, our method achieves the same performance as text detectors trained with polygon annotations (i.e., both are 85.0% F-score for PSENet on ICDAR2015). For DST, through dynamically removing the false alarms, it is able to leverage limited labeled data as well as massive unlabeled data to further outperform the expensive baseline. We hope SBP can provide a new perspective for text detection to save huge labeling costs. Code is available at: [github.com/weijiawu/SBP](https://github.com/weijiawu/SBP).

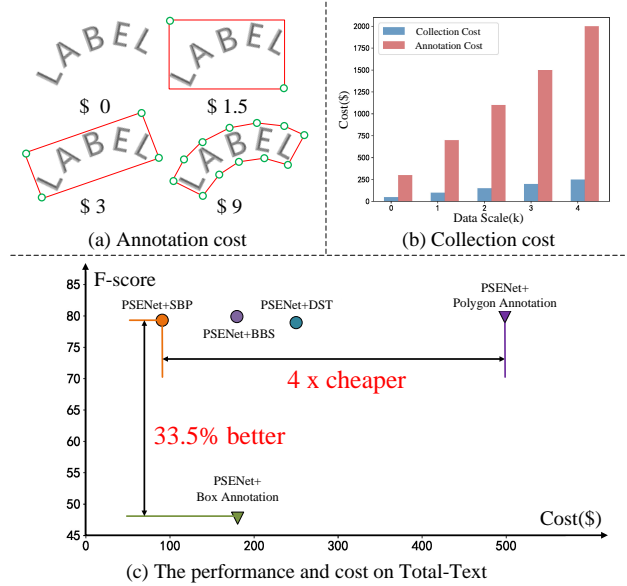


**Figure 1** – The comparisons of data cost and the performance of the proposed method. (a) Annotating more points are more expensive (the price of 100 text instances). (b) Data collection is much cheaper than annotation. (c) The proposed SBP achieves competitive performance while saving huge labeling costs for PSENet [30] on Total-Text [4]. Note that the data cost information is obtained from Amazon Mechanical Turk (MTurk), and we make a rough cost evaluation of Total-Text.

## 1. Introduction

Scene text detection [28, 16, 40, 21, 22], which aims to locate texts in the wild, has achieved much attention in recent years because of its numerous applications, e.g., in-

stant translation, image retrieval, scene parsing. Since text instances in the real-world scenario are usually with various sizes, directions and shapes, most scene text detection methods [30, 21, 31] utilize polygon annotation to train robust text detectors. Although the polygon is more accurate than the upright bounding box (bounding box equals upright bounding box with two points in this paper), the labeling cost of polygons is extremely high, limiting its large-scale extension in real-world applications.

To address the above-mentioned issue, in this paper, we propose a novel system termed *SelfText Beyond Polygon (SBP)* for unconstrained scene text detection with ex-

<sup>1</sup> Zhejiang University, China.

<sup>2</sup> The University of Hong Kong, Hong Kong SAR.

<sup>3</sup> Nanjing University, China.

<sup>4</sup> Facebook AI, USA.

<sup>5</sup> Chinese University of Hong Kong, Shenzhen.

<sup>†</sup> Corresponding author. (zhouh@mail.bme.zju.edu.cn)

\* Authors contributed equally. (wwj123@zju.edu.cn)

tremely low data collection and labeling costs, *i.e.*, with limited bounding box annotated data and a larger amount of unlabeled data. Our motivations are inspired by the following observations. **First**, although bounding box annotation is limited by its performance, there is still a cheap way of labeling to roughly distinguish the foreground and background locations. As illustrated in Fig. 1 (a), according to the Amazon Mechanical Turk (MTurk), the upright bounding box annotations are about  $4\times$  cheaper than polygon annotations [4, 38]. Thus, how to effectively utilize the bounding box annotations to boost the detection accuracy becomes critical in such a situation. **Second**, even if the upright bounding box annotation is adopted, the cost is still very high when the data volume breakthroughs the million range. Fortunately, the data collection cost is usually much cheaper than labeling with the amount of the data increases, just as shown in Fig. 1 (b). Thus how to progressively mining the valuable information hidden in the massive unlabeled data to further improve the accuracy of the detector is another problem that will be addressed in this paper.

In practice, we deal with the above problems by proposing two novel schemes named Bounding Box Supervision (BBS) and Dynamic Self-Training (DST) to efficiently use a limited set of bounding-box annotated data and massive unlabeled data, respectively. **For the former one**, we firstly apply the synthetic data whose character-level annotations can be automatically generated for free, to pre-train a newly proposed Skeleton Attention Segmentation Network (SASN). By exploiting the text data with various geometric information (*e.g.*, the straight and the curved data) in the training phase, the SASN could effectively capture the changes of the text appearance in different scenes. Then bounding box annotations are used to crop the text region in the real images which are fed into SASN to generate high-quality polygon-like pseudo labels. By splicing all of these local pseudo labels, the global one would be obtained and applied to train any text detectors. **For the later one**, we propose a Dynamic Self-Training (DST) scheme, which adopts the filtering and multi-scale inference strategies to reduce the effect of false positive and false negative in pseudo labels for the unlabeled data. In addition, the dynamic mixed training strategy is also used to limit the use of the pseudo labels in the late stage of training. As shown in Fig. 1 (c), by using BBS and DST, PSENet [30] achieves  $4\times$  cheaper data cost compare with that of using polygon annotation, and obtaining 33.5% F-score improvements compare with that of directly using bounding box annotation on Total-Text [4]. The main contributions are four folds:

(1) We introduce a Bounding Box Supervision strategy, which utilizes free synthetic data and box-level annotations to achieve high quality polygon-like real annotations (*i.e.*, pseudo labels).

(2) We introduce a Skeleton Attention Segmentation

Network for capturing the structure of the texts with arbitrary shapes and restraining noise interference.

(3) We propose a stable self training scheme termed Dynamic Self-Training to utilize large scale unlabeled data and limited labeled data for robust detectors training.

(4) The proposed SelfText Beyond Polygon is simple but surprisingly effective and practical, which saves **70%+**(rough estimation) cost and achieves almost the same performance compared with fully-supervised methods.

## 2. Related Work

### 2.1. Supervised Text Detection

Scene text detection has achieved remarkable progress in the deep learning era. Previous methods [16, 39] focused on horizontal text detection. CTPN [28] adopted Faster RCNN [26] and modified RPN to detect texts. Then many famous methods [23, 17] aim at solving multi-oriented text detection. EAST [40] used FCN [19] to predict text score map, distance map and angle map in an anchor-free manner. Recent works focus on curved text detection [1, 35]. TextSnake [21] modeled curved text instance as a series of ordered disks and a text center line. SPCNet [33] and Mask Text Spotter [22] are based on Mask RCNN, which translate curved text detection as a instance segmentation problem. PSENet [30] and PAN [31] treat text instance as kernels with different scales, and reconstruct the whole text instance in the post-processing.

### 2.2. Weak Supervised Object Detection

To alleviate the expensive data cost problem, there have been various weakly supervised object detection (WSOD) works [29] based on image-level annotations. Bilen *et al.* [2] proposed an architecture called WSDDN to select and classify region proposals simultaneously. ContextLocNet [12] further improves WSDDN by taking contextual region into consideration. Beyond that, some works tried to utilize the temporal information in videos. Kwak *et al.* [15] discovered object appearance representation across videos and tracked the object in temporal space for supervision. Wang *et al.* [32] performed unsupervised tracking on videos and clustered similar features. Recently, Yang *et al.* [36] and Kim *et al.* [14] proposed activity-driven methods, which exploits action classes as contextual information to localize objects. Different from the above methods, we develop a novel pipeline for weakly supervised text detection, which generating polygon-like pseudo label with bounding-box annotation (2 points) instead of polygon annotation (4-20 points) to train networks.

### 2.3. Self-training with noisy labels

Self-training, where a teacher model is used to generate labels for the unlabeled set the student can train on, is

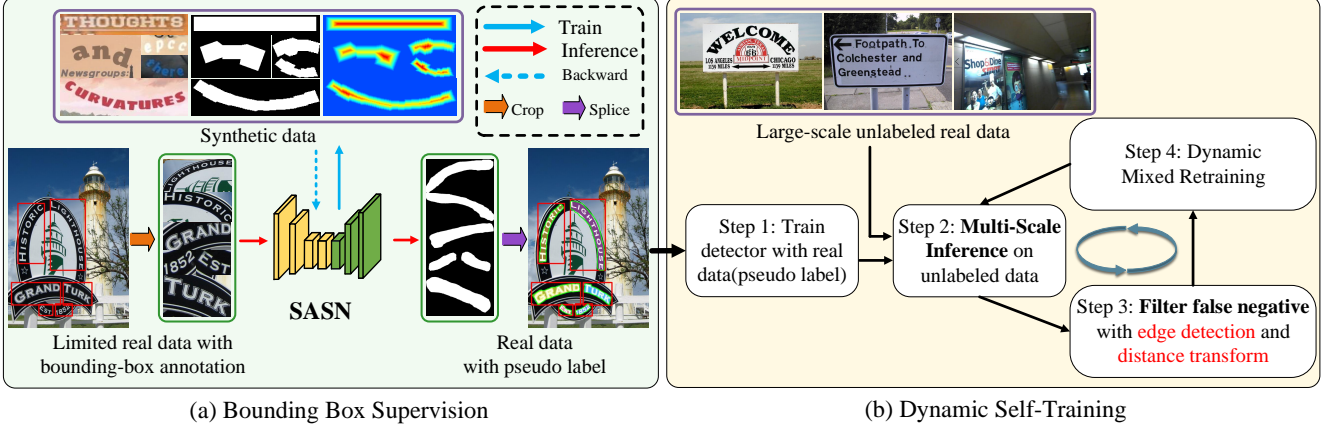


**Figure 2** – Illustration of the whole SelfText Beyond Polygon. (a) The pipeline of the Bounding Box Supervision, which training with synthetic data and inference on real data to generated pseudo label, details as shown in Fig. 3. (b) The pipeline of Dynamic Self-Training, which utilizes limited data and massive unlabeled data to train detectors for saving cost.

a widely-used methods in semi-supervised learning. Xie *et al.* [34] use strong data augmentation in self-training but only for image classification. Ilija *et al.* [25] proposed a data distillation method to improve instance detection level tasks and vote on unlabeled data to get pseudo-label. Recently, noise labels have been shown to have positive effects in self-training for object detection [41], which motivates our work. In this work, we introduce a novel dynamic self-training approach to minimizing the negative effects of false negatives and false positives in pseudo labels.

### 3. Methods

As shown in Fig. 2, we describe the details of the proposed SelfText Beyond Polygon (SBP), which has two key components termed the Bounding Box Supervision (BBS) and the Dynamic Self-Training (DST).

#### 3.1. Bounding Box Supervision

Following the segmentation with bounding boxes [6], we propose a weakly supervised method, termed Bounding Box Supervision (BBS), which can achieve competitive accuracy with low-cost bounding box annotations for text detection. As shown in Fig. 2 (a), BBS utilizes a novel proposed Skeleton Attention Segmentation Network (SASN), which is shown in Fig. 3, to generate polygon pseudo labels based on the given bounding box annotations. The process composes three steps. (1) In the first step ( see blue arrows in Fig. 2 ), we train SASN with free synthetic data based on character annotation. (2) In the second step ( see red arrows in Fig. 2 ), the box-level annotations are utilized to crop the real image, which are fed into the SASN for generating polygon-like pseudo labels. (3) By splicing all of the local pseudo labels, the global one is obtained. In this way, bounding box annotations can be converted to high-quality polygon pseudo labels. The detectors ( e.g., PSENet [30] )

trained on these pseudo labels can achieve almost the same performance as those trained on polygon annotations.

##### 3.1.1 Skeleton Attention Segmentation Network

**Network Architecture.** As presented in Fig. 3 (a), we use ResNet50 [11] as the backbone network for the SASN, and extract three levels of features ( *i.e.*,  $C1, C2, C3$  ) from different downsampled scales ( *i.e.*,  $1/4, 1/8, 1/16$  ). After that, the skeleton stream fuses  $C1$  and  $C3$  to predict the skeleton attention map. At the same time, the regular stream segment the text by applying the Skeleton Attention Module. Although text segmentation in a bounding box is easier than in the whole image, there still exists a bit of noise. For example two texts in one bounding box, which is illustrated in the Fig. 3 (a) with green circle. To restrain the noise interference and segment the body text precisely, we carefully design the Skeleton Attention Module, which generates the skeleton map to drive the attention mechanism.

**Skeleton Attention.** Fig. 3 (b) illustrates the details of the Skeleton Attention Module (SA). Given an input sample  $(x_i, y_i) \in \{(x_1, y_1), (x_2, y_2), \dots, (x_n, y_n)\}$ , where  $x_i$  and  $y_i$  denote the  $i$ -th image and its labels. We use  $x_i^k$  to denote the  $k$ -th pixel of the  $i$ -th training image, with  $y_i^k = 0$  for the background and  $y_i^k = 1$  for the text pixel. We also define the text skeleton ground-truth as a soft label. For the  $k$ -th pixel in the text region of  $i$ -th image, we first calculate the shortest distance  $d_i^k$  between the  $k$ -th pixel to its nearest background pixel, and then the value  $p_i^k$  is defined as the soft skeleton label of  $k$ -th pixel by normalizing  $d_i^k$  to  $[0, 1]$ :

$$p_i^k = \sum_k \frac{d_i^k}{d_i^*}, \quad (1)$$

where  $d_i^*$  is the maximum value of  $\{d_i^k\}$  in the  $i$ -th image.

Intuitively, the pixels close to the skeleton of the text instance should have a greater value than the boundary pixels (

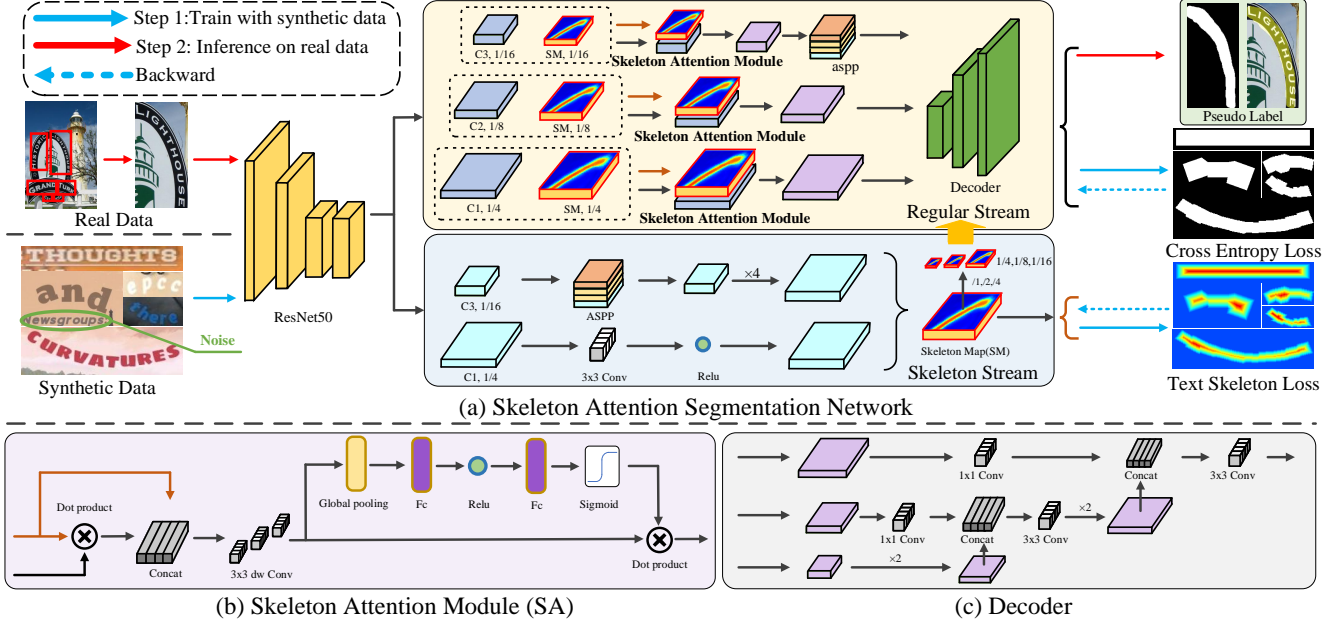


**Figure 3** – The whole pipeline of Bounding Box Supervision. (a) The architecture of Skeleton Attention Segmentation Network, which is composed of two streams: regular stream and skeleton stream. (b) The details of Skeleton Attention Module, which refine the input feature map by weighting with attention map. (c) The detailed structure of the Decoder. How to generate polygon-like pseudo label includes two steps: (1) Blue arrows show training SASN with synthetic data based on character annotations. (2) Red arrows illustrate generating pseudo labels on real data based on bounding box annotations.

see text skeleton label in Fig. 3 (a) ). Since the soft label is a decimal representing the degree of distance, it is incompatible with the commonly binary cross-entropy loss. Besides, L1 and L2 loss are not sensitive to the distance distribution among  $[0, 1]$  [26]. Therefore, to handle the soft label, we modify the cross-entropy loss into a “soft” form. For a pixel  $x_i^k$ ,  $p_i^k$  denotes the value of the  $k$ -th pixel in the ground truth skeleton map.  $\mathcal{F}$  indicates neural networks. Thus the text skeleton loss in Fig. 3 (a) is defined as follows:

$$\mathcal{L}_{ske} = - \sum_k \log(1 - |p_i^k - \mathcal{F}(x_i^k)|). \quad (2)$$

In practice, the predicted skeleton map is downsampled to obtain multi-scale maps (*i.e.*, 1/4, 1/8, 1/16), which are transferred to the regular stream (the thick yellow arrow in Fig. 3 (a) ). And then, the extracted feature map (*e.g.*,  $C1$ ) and the corresponding scale skeleton map are as the input of the Skeleton Attention Module. The two feature maps before and after the skeleton attention are concatenated and fed into a channel attention block. At last, it outputs the refined feature map. Note that the proposed Skeleton Attention Module is shared for the high-level and the low-level feature maps (*i.e.*,  $C1, C2, C3$  ).

### 3.1.2 Suitable Synthetic Datasets

Existing real-world text datasets can be divided two types: straight (*e.g.*, ICDAR2015 [13]) and curved (*e.g.*, Total-

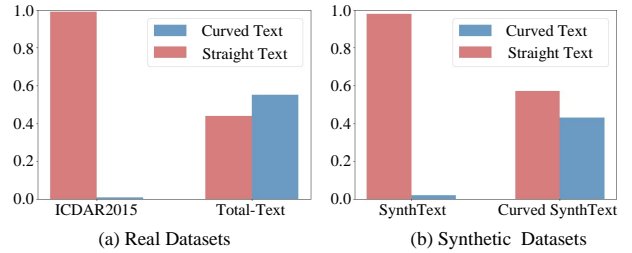


**Figure 4** – The shape distribution difference between synthetic data and real data causes serious domain gap.

Text [4]), depending on the shape of the text instance. However, the curved synthetic text data is scarce. SynthText [9], the most widely-used synthetic datasets, does not contain curved text, which leads to a serious domain gap between synthetic data and real data (*e.g.*, Total-Text) in curved text distribution ( 0.2% *v.s.* 58% ), as shown in Fig. 4. Therefore, we also adopt Curved SynthText [20] to align the data distribution with curved dataset. In this work, we use SynthText [9] to train SASN for straight text line and use Curved SynthText [20] to match curved text line.

### 3.2. Dynamic Self Training for Text Detection

Inspired by previous works [34, 41], we propose a novel self-training strategy, termed Dynamic Self Training, to reduce label cost by exploiting large-scale unlabeled data.



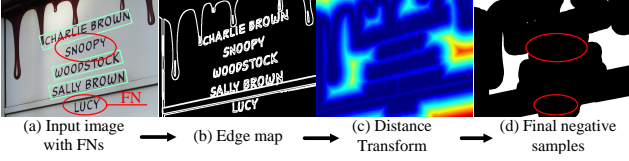


**Figure 5** – Background Filtering Process. (a) The pseudo labels contains False Negatives. (b) Generated edge map by edge detector ( *i.e.*, Canny [8] ). (c) Generated distance map by using Distance Transform. (d) The final refined negative samples ( *i.e.*, white regions ).

### 3.2.1 Overview of Dynamic Self-Training

Fig. 2 (b) gives an overview of the proposed dynamic self-training scheme. In such case, we have a large set of unlabeled images  $\{\tilde{x}_i\}_{i=1}^m$  and limited labeled images  $\{(x_j, y_j)\}_{j=1}^n$ . Here  $y_i$  could indicate the polygon-like label generated from BBS or the manually labeled ground truth. We firstly use the labeled images to train an initial detector  $\theta$ . Then we apply the detector  $\theta$  to generate multi-scale prediction results  $\{\tilde{y}_i\}_{i=1}^m$  as the foreground maps of unlabeled images  $\{\tilde{x}_i\}_{i=1}^m$ . When  $\{\tilde{y}_i\}_{i=1}^m$  is obtained, we can further calculate the background maps  $\{\tilde{z}_i\}_{i=1}^m$  by filtering false negatives, as shown in Fig. 5. Specifically, false negatives is filtered by thresholding the distance score  $\tilde{t}_i^k$  of each negative sample pixel, which is calculated by a distance transform function  $D(\cdot)$  [3] and edge detection  $E(\cdot)$  ( *i.e.*, Canny [8] ). By leveraging the information from  $\{\tilde{y}_i\}_{i=1}^m$  and  $\{\tilde{z}_i\}_{i=1}^m$ , we could generate the high-quality pseudo label for unlabeled data. Please refer to Sec. 3.2.2 for more details. After that, we conduct the dynamic mixed retraining of the model by using both  $\{(\tilde{x}_i, \tilde{y}_i, \tilde{z}_i)\}_{i=1}^m$  and  $\{(x_j, y_j)\}_{j=1}^n$ , and adaptively adjust the number of the unlabeled data in a mini-batch. Sec. 3.2.3 gives the detailed training process.

Algorithm 1 summarizes the scheme of DST.  $E(\cdot)$  represents gradient edge detector [8], which is utilized to filter text region with regular change of gradient.  $D(\cdot)$  represents a distance transform function [3].  $M(\cdot)$  and  $\phi$  refer to the multi-scale inference and the scale set, respectively. The shortest distance  $\tilde{t}_i^k$  between  $k$ -th pixel and gradient edge ( *i.e.*, the white line in Fig. 5 (b) ) can be calculated by the distance transform function. The pixel with bigger  $\tilde{t}_i^k$  is usually farther from gradient edge, leading to the lower probability to be the foreground.

### 3.2.2 High-quality Pseudo Label Generation

**Multi-Scale Inference.** As shown in Algorithm 1, we use multi-scale inference to exploit hard positive samples as many as possible. When generating pseudo labels  $\{\tilde{y}_i\}_{i=1}^m$ , the unlabeled image is resized to a pre-defined set of scales  $\phi = \{\varepsilon - 3\psi, \varepsilon - 2\psi, \varepsilon - \psi, \varepsilon, \varepsilon + \psi, \varepsilon + 2\psi, \varepsilon + 3\psi\}$  to generate multi-scale predictions, where  $\varepsilon$  denotes the shorter side of an image and  $\psi$  is set as 32 in prac-

---

#### Algorithm 1: Dynamic Self-Training Method.

---

**Input:** Labeled images

$(x_1, y_1), (x_2, y_2), \dots, (x_n, y_n)$   
 unlabeled images  $\tilde{x}_1, \tilde{x}_2, \dots, \tilde{x}_m$   
 multi-scale  $s_1, s_2, \dots, s_t$

**Output:** trained parameters  $\theta$

---

training the model  $\theta$  on

$(x_1, y_1), (x_2, y_2), \dots, (x_n, y_n)$  (just as in normal supervised learning)

**while** *epoch* **do**

    multi-scale inference  $\tilde{y}_i \leftarrow M(f(\tilde{x}_i|\phi, \theta))$

    compute edge map  $e_i \leftarrow E(\tilde{x}_i)$

    compute distance map  $\tilde{t}_i^k \leftarrow D(1 - e_i)$

    filtering negative samples  $\tilde{z}_i$

**if**  $\tilde{t}_i^k > \sigma$  **then**

$\tilde{z}_i \leftarrow 1$ ;

**else**

$\tilde{z}_i \leftarrow 0$ ;

**end**

    dynamic mixed retraining model  $\theta$  on the union  
     of  $(x_1, y_1), (x_2, y_2), \dots, (x_n, y_n)$  and  
      $(\tilde{x}_1, \tilde{y}_1, \tilde{z}_1), (\tilde{x}_2, \tilde{y}_2, \tilde{z}_2), \dots, (\tilde{x}_m, \tilde{y}_m, \tilde{z}_m)$

**end**

---

tice. And then, the Locality-Aware NMS [40] is used to ensemble the multi-scale inference results of each unlabeled image. Such aggregating scheme often obtains a prediction that is always superior to any of the model’s predictions under a single scale, especially for most text detectors without FPN [18].

**Filtering Negative Samples.** To obtain the accurate background maps  $\{\tilde{z}_i\}_{i=1}^m$ , we need to identify and discard the false negative regions. In consideration of the particularity of text, we use the edge detection and distance transform to filter pixels and select the ones far away from the gradients of image as the final background pixels. As shown in Fig. 5, for an input image  $\tilde{x}_i$ , we firstly obtain the corresponding edge map by edge detector. And then, the distance transform ( *i.e.*,  $D(\cdot)$  in Algorithm 1 ) is used to calculated the distance  $\tilde{t}_i^k$  between  $k$ -th pixel and  $b$ -th pixel, where  $b$ -th pixel is the nearest one of  $k$ -th pixel on gradient edge ( *i.e.*, the white parts in Fig. 5 (b) ). Similar to Eqn. 1, the  $\tilde{t}_i^k$  is normalized to  $[0, 1]$ , and Fig. 5 (c) presents the visualization of the distance map. Finally, the background maps  $\{\tilde{z}_i\}$  are calculated by thresholding the score map  $\{\tilde{t}_i^k\}$  with a lower threshold  $\sigma$ , which is set as 0.1 in all of the experiments.

### 3.2.3 Dynamic Mixed Training

The generated pseudo labels usually contain false positive (FP) and false negative (FN), which causes unsteady con-

Synthetic Data	Size	Evaluation on Total-Text/%		
		Precision	Recall	F-score
SynthText	50k	78.3	73.5	75.9
SynthText	500k	<b>80.3</b>	<b>73.5</b>	<b>76.8</b>
SynthText	1m	79.7	74.0	76.7
Curved SynthText	50k	80.8	75.0	77.8
Curved SynthText	500k	<b>81.7</b>	<b>75.6</b>	<b>78.5</b>
Curved SynthText	1m	81.3	75.1	78.1

**Table 1 – Synthetic Data for BBS:** suitable annotation method bring a large gain. The Skeleton Attention and PSENet [30] are used in the experiment.

vergence of network. To tackle this problem and making full use of unlabeled data, we propose the dynamic mixed training, which optimizes models with more unlabeled data ( *e.g.*, 28 unlabeled images and 6 labeled images ) in the early stage of training, and utilize more unlabeled data in the later stage. In the training stage, a batch size data with the volume  $\tau$  is composed of  $\alpha$  labeled images and  $\beta$  unlabeled images, where  $\beta + \alpha = \tau$ . Here  $\alpha$  can be calculated with the formula,  $\alpha = \frac{\text{current epoch}}{\text{max epoch}} * \tau$ . The loss function in each iteration can be written as:

$$\mathcal{L}_{dmt} = \frac{1}{\alpha} \sum_{j=1}^{\alpha} \mathcal{L}_1(y_j, \mathcal{G}(x_j, \theta)) + \frac{1}{\beta} \sum_{i=1}^{\beta} \mathcal{L}_2(\tilde{y}_i, \tilde{z}_i, \mathcal{G}(\tilde{x}_i, \theta)), \quad (3)$$

where  $\mathcal{G}$  denotes the text detector.  $\mathcal{L}_1(\cdot)$  and  $\mathcal{L}_2(\cdot)$  denotes corresponding loss of detector on labeled data and pseudo labeled data, respectively.

## 4. Experiments

### 4.1. Datasets and Experimental Settings

**Pure Synthetic Datasets.** *SynthText* [9] consist of 800k synthetic images generated by adding variants of multi-oriented text with random fonts, size, and color. *Curved SynthText*<sup>1</sup> [20] generates 80m curved texts with character level annotation by revising the text rendering module of the SynthText engine.

**Real Datasets.** *ICDAR2015* [13] includes 1,000 training and 500 testing images with quadrilateral annotation. *Total-Text*[5] is a English curved text dataset contains 1,555 images, which includes 3 different text orientations: horizontal, multioriented, and curved. *MSRA-TD500* [37] consists of 500 training and 200 testing images for detecting multi-lingual long texts of arbitrary orientation. *ICDAR2017-MLT* [24] consists of 18000 images with texts in 9 languages for multi-lingual text detection.

**Implementation Details.** *Bounding Box Supervision.* All of the experiments use the same strategy: (1) training SASN with synthetic data based on character annotation.

<sup>1</sup><https://github.com/PkuDavidGuan/CurvedSynthText>

Method	Synthetic Data	Evaluation on Total-Text/%		
		Precision	Recall	F-score
Baseline	SynthText(500k)	77.2	73.0	75.0
Baseline+SA	SynthText(500k)	<b>80.3</b>	<b>73.5</b>	<b>76.8</b>
Baseline	Curved SynthText(500k)	80.5	73.2	76.7
Baseline+SA	Curved SynthText(500k)	<b>81.7</b>	<b>75.6</b>	<b>78.5</b>

**Table 2 – Skeleton Attention:** SA bring a large gain regardless of dataset. The ‘SA’ denotes the ‘Skeleton Attention’. PSENet [30] is adopted as the detector.

Method	Evaluation on ICDAR2015/%		
	Precision	Recall	F-score
Baseline	59.2	59.3	59.2
Baseline,ST	70.1	67.3	68.6
Baseline,ST,Iter	70.8	68.1	69.2
Baseline,ST,Iter,DM	71.2	68.5	69.8
Baseline,ST,Iter,DM,DS	72.5	70.1	71.3
Baseline,ST,Iter,DM,DS,Fil	<b>73.7</b>	<b>69.9</b>	<b>71.7</b>

**Table 3 – Ablation study of DST:** we use PSENet [30] as the base detector, and randomly split the ICDAR2015 training set into 100 labeled and 900 unlabeled images. ‘Baseline’ and ‘ST’ denote ‘training with only labeled data’ and ‘self-training on unlabeled data’, respectively. ‘DM’, ‘DS’, ‘Fil’, ‘Iter’ denote ‘dynamic mixed training’, ‘multi-scale inference’, ‘filtering’ and ‘iterative self-training’, respectively.

(2) generating the pixel level pseudo label on real data based on bounding box annotation with SASN. (3) training the detectors (*i.e.*, EAST and PSENet) with the pseudo label. The stochastic gradient descent(SGD) optimizer is adopted with a momentum of 0.9 and a weight decay of 0.0005. The batch size is set to 8 per GPU. The learning rate is initialized to 0.02 and decayed with the power of 0.9 for 16 epochs. During training and inference, the crop images are resized to a resolution of  $128 \times 128$ . *Dynamic Self-Training.* All of the experiments use the same training strategy: (1) we firstly choose a part of training data as labeled data to train the detectors. (2) generating pseudo label in the rest of the data with the proposed components. (3) fine-tune the detectors on whole data. To evaluate the effectiveness of the DST, we randomly split the training set into labeled data and unlabeled data, and using one ratio control the labeled data size in the total training set. PSENet [30] and EAST [40] are adopted as the base detectors because of the popularity. While involving PSENet [30] and EAST [40] experiments, all settings are following the original paper.

### 4.2. Ablation Study

In this part, we conduct three groups ablation experiments to analyze BBS and DST. More ablation (*e.g.*, Box supervision v.s. Strong supervision, Labeled data size for DST) experiments are in supplementary materials.

**Synthetic data for BBS.** To understand the impact of synthetic data with different text shape distribution, we compare the performance of curved Synthtext [20] and Synthtext [10]. As shown in Tab. 1, using curved Synthtext obtains better performance, 2% absolute improvement over

Method	Annotation	Pre	ICDAR2015/%			MSRA-TD500/%			ICDAR2017-MLT/%			Total-Text/%			
			P	R	F	P	R	F	P	R	F	P	R	F	
<i>Strong Supervision</i>															
CTPN[28]	GT	-	74.2	51.6	60.9	-	-	-	-	-	-	-	-	-	
SegLink[27]	GT	✓	73.1	76.8	75.0	86.0	70.0	77.0	-	-	-	30.3	23.8	26.7	
EAST[40]	GT	-	80.5	72.8	76.4	81.7	61.6	70.2	-	-	-	-	-	-	
PixelLink[7]	GT	-	82.9	81.7	82.3	83.0	73.2	77.8	-	-	-	-	-	-	
TextSnake[21]	GT	✓	84.9	80.4	82.6	83.2	73.9	78.3	-	-	-	82.7	74.5	78.4	
PSENet[30]	GT	-	81.5	79.7	80.6	-	-	-	73.7	68.2	70.8	81.8	75.1	78.3	
PSENet[30]	GT	✓	86.9	84.5	85.7	-	-	-	-	-	-	84.0	78.0	80.9	
EAST <sup>†</sup>	GT	-	76.9	77.1	77.0	71.8	69.1	70.4	68.1	63.2	65.6	-	-	-	
EAST <sup>†</sup>	GT	✓	82.0	82.4	82.2	77.9	76.5	77.2	70.3	62.8	66.4	-	-	-	
PSENet <sup>†</sup>	GT	-	81.6	79.5	80.5	80.6	77.7	79.1	73.1	67.3	70.1	80.4	76.5	78.4	
PSENet <sup>†</sup>	GT	✓	86.4	83.5	85.0	84.1	85.0	84.5	72.5	69.1	70.8	83.4	78.1	80.7	
<i>Box Supervision</i>															
EAST <sup>†</sup>	b-GT	-	65.8	63.8	64.8	40.5	31.1	35.2	66.3	59.6	62.8	-	-	-	
EAST <sup>†</sup> +BBS	PL	-	77.8	78.2	78.0	71.3	70.2	70.7	67.3	64.1	65.7	-	-	-	
EAST <sup>†</sup>	b-GT	✓	70.8	72.0	71.4	48.3	42.4	45.2	67.2	60.1	63.5	-	-	-	
EAST <sup>†</sup> +BBS	PL	✓	81.3	82.2	81.8	77.4	75.5	76.4	67.6	64.9	66.3	-	-	-	
PSENet <sup>†</sup>	b-GT	-	70.2	69.1	69.6	47.2	36.9	41.4	67.2	61.4	64.2	46.5	43.6	45.0	
PSENet <sup>†</sup> +BBS	PL	-	82.9	77.6	80.2	80.3	77.5	78.9	72.4	69.3	70.8	81.7	75.6	78.5	
PSENet <sup>†</sup>	b-GT	✓	72.7	74.3	73.5	47.5	39.5	43.1	66.4	63.1	64.7	51.9	47.5	49.6	
PSENet <sup>†</sup> +BBS	PL	✓	86.8	83.3	85.0	84.4	84.7	84.5	73.8	67.7	70.6	82.5	77.6	80.1	

**Table 4** – The results of BBS on ICDAR2015, MSRA-TD500, ICDAR2017-MLT, Total-Text. <sup>†</sup> refers to our testing performance. The ‘GT’, ‘b-GT’, ‘PL’ refer to the ‘Ground Truth’, ‘Bounding-box annotation of ground truth’, ‘Pseudo Label generated by the SASN training on SynthText [10] or curved SynthText [20]’. ‘P’, ‘R’, ‘F’ and ‘Pre’ refer to ‘Precision’, ‘Recall’, ‘F-score’ and ‘pretraining on external data’, respectively. In green and in bold are highlighted for comparison.

that using Synthtext, because of the serious domain gap of text shape between Total-Text (curved text) and Synthtext (straight text). The performance tends to stabilize while synthetic data size exceeds 500k, so we randomly select 500k synthetic data to train SASN in all experiments.

**Skeleton Attention for BBS.** Skeleton Attention is the key to the SASN. Tab. 2 gives the ablation study about the attention on Total-Text [4]. No matter which synthetic data, Skeleton Attention can obtain up to 2% improvement compares to the baseline without the attention. In addition, Fig. 6 gives the visualization of the attention map, which enables the network more interested in the text skeleton.

**Components for DST.** Dynamic mixed training, multi-scale inference and filtering are the keys for DST. We make an assumption that these components independent of each other, which improve the performance of model from different levels by minimizing the effects of false negatives and false positives. Tab. 3 also indirectly proves the conclusion. By combining with dynamic mixed training, multi-scale inference and filtering, the F-score achieved a 69.8%, 71.3% and 71.7%, respectively, making 0.6%, 0.5% and 0.4% absolute improvements over the baseline.

### 4.3. Experiments on Scene Text Detection

In this section, we firstly present the experiments of BBS and DST, respectively. And then, the combined experiments are given in supplementary materials.

#### 4.3.1 Bounding Box Supervision

**Quadrilateral-type datasets.** Tab. 4 lists the experimental results of various methods on ICDAR2015, ICDAR2017 and MSRA-TD500 datasets. For *ICDAR2015*, PSENet [30] using pseudo label achieves **almost the same performance** (80.2% and 85.0% using the pre-trained model on SynthText) with that using ground truth, which prove high-quality of pseudo label generated by BBS. On the contrary, directly training the detector with bounding box annotation has an unsatisfactory F-score (69.6% and 73.5%), which exists more than 10% gap compare with that using polygon annotation. EAST [40] has a similar case with PSENet. Moreover, the F-score (78.0%) of using the pseudo label has a 1.0% improvement over that (77.0%) of using ground truth. For *MSRA-TD500*, annotations are provided at the line level, including the spaces between words in the box. Therefore, bounding box annotation on MSRA-TD500 usually contains large plenty of background, which causes **poor performance** (35.2% for EAST and 41.4% for PSENet). In this case, the pseudo label from BBS still brings almost the same performance (70.7% for EAST and 78.9% for PSENet) with that (70.4% for EAST and 79.1% for PSENet) of polygon annotation. In addition, after using the pre-trained model on SynthText, PSENet and EAST all obtain almost the same improvement no matter using which labels (pseudo label or ground truth). For *ICDAR2017*, the performance is similar to ICDAR15, pseudo label has a high-quality performance compare with that using ground

Method	Ratio	Pre	ICDAR2015/%		
			P	R	F
<i>Strong Supervision</i>					
EAST <sup>†</sup>	100%	-	76.9	77.1	77.0
EAST <sup>†</sup>	100%	✓	82.0	82.4	82.2
PSENet <sup>†</sup>	100%	-	81.6	79.5	80.5
PSENet <sup>†</sup>	100%	✓	86.4	83.5	85.0
<i>Self-Training</i>					
EAST <sup>†</sup>	50%	-	77.1	75.7	76.4
EAST <sup>†</sup> +DST	50%	-	77.6	77.5	77.5 (+1.1)
EAST <sup>†</sup>	50%	✓	79.1	79.2	79.1
EAST <sup>†</sup> +DST	50%	✓	82.6	79.7	81.1 (+2.0)
PSENet <sup>†</sup>	50%	-	76.6	73.6	75.1
PSENet <sup>†</sup> +DST	50%	-	79.8	76.8	78.3 (+3.2)
PSENet <sup>†</sup>	50%	✓	78.9	76.6	77.7
PSENet <sup>†</sup> +DST	50%	✓	84.0	82.9	83.5 (+5.8)

**Table 5** – The results of DST on ICDAR2015. ‘Ratio’, ‘P’, ‘R’, and ‘F’ refer to ‘the proportion of using labeled data’, ‘Precision’, ‘Recall’ and ‘F-score’, respectively. In blue are the gaps of at least (+1.1) point.

Method	Ratio	Pre	ICDAR2017-MLT/%		
			P	R	F
<i>Strong Supervision</i>					
EAST <sup>†</sup>	100%	-	68.1	63.2	65.6
PSENet <sup>†</sup>	100%	-	73.1	67.3	70.1
<i>Self-Training</i>					
EAST <sup>†</sup>	50%	-	70.4	60.2	64.5
EAST <sup>†</sup> +DST	50%	-	69.2	63.5	66.2 (+1.7)
PSENet <sup>†</sup>	50%	-	69.1	68.4	68.7
PSENet <sup>†</sup> +DST	50%	-	70.6	69.8	70.2 (+1.5)

**Table 6** – The results of DST on ICDAR2017-MLT. ‘Ratio’, ‘P’, ‘R’, and ‘F’ refer to ‘the proportion of using labeled data’, ‘Precision’, ‘Recall’ and ‘F-score’, respectively. In blue are the gaps of at least (+1.5) point.

truth. The difference is that the bounding box also brings relatively good performance (62.8% for EAST and 64.2% for PSENet). The main reason is that texts in ICDAR17 have a small tilting angle and size.

**Polygon-type dataset.** Tab. 4 lists the experimental results on Total-Text [4]. The annotation on Total-Text is complex and polygonal in shape. The **great performance** (78.5%) of using pseudo label further proves the significance of our work, and Fig. 7 gives some visualization of ground truth and pseudo label. Similar to MSRA-TD500, bounding box annotation on Total-Text also contains plenty of backgrounds, which causes poor performance (45.0% and 49.6%). And using the pseudo label generated by BBS still can achieve a great performance (78.5% and 80.1%) with 33.5% and 30.5% improvements.

### 4.3.2 Dynamic Self Training

We present the experimental results on ICDARs in this subsection, and more experiments(*i.e.*, Total-Text) are in the supplementary material. For ICDAR2015, Tab. 5 lists the experimental results of the self-training, and the ‘Ratio’ de-

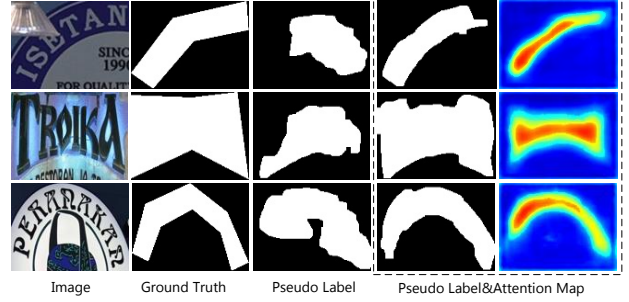


**Figure 6** – The visualization of BBS on Skeleton Attention. The Skeleton Attention enables the network to focus on the skeleton of body text instance for segmenting precisely.



**Figure 7** – The visualization of bounding-box annotation and the pseudo labels generated by BBS on Total-Text [4].

notes only using part of training set as the labeled data. By using DST, EAST using half labeled data and half unlabeled data obtains the **great performance** (77.5% *v.s.* 77.0% and 81.1% *v.s.* 82.2%), which is almost the same as that of strong supervision. After using the pre-trained model on SynthText, the performance can be further improved with 2.0% gap. Similar to EAST, PSENet also has achieved a **competitive performance** (78.3% *v.s.* 80.5% and 83.5% *v.s.* 85.0%) with only half labeled training set. For ICDAR2017, Tab. 6 lists the experimental results of the self-training. Similar to ICDAR15, our method all achieve competitive performance (66.2% *v.s.* 65.6.0% and 70.2% *v.s.* 70.1%) no matter which detectors are used.

## 5. Conclusion

In this paper, we present a simple but surprisingly effective and practical method termed SelfText Beyond Polygon (SBP), which includes two components: Bounding Box Supervision (BBS) and Dynamic Self-Training (DST). The BBS with only bounding box annotation achieve almost the same performance as using expensive polygon annotation. The DST training with limited labeled data and unlabeled data to further reduce the data cost. The experiments showed that our method achieves almost the same performance as that of strong supervision while saving 70%+ data cost, which can provide a new perspective for weakly supervised text detection and save much money for the industry.



## 6. Appendix

### 6.1. More Analysis for Dynamic Mixed Training

As shown in Fig. 8, fully supervision (green line) usually has a stable convergence effect ( $\pm 0.2\%$ ), normal self-training (red line) has a performance fluctuation ( $\pm 2.0\%$ ), because of the adverse effects of false negatives (FNs) and false positives (FPs). Fortunately, Dynamic Mixed Training could achieve competitive convergence performance ( $\pm 0.8\%$ ) by dynamically adjusting the number of unlabeled data in a mini-batch, as shown in the blue line. The basic idea is simple but effective, the network training with few unlabeled data for minimizing the adverse effects of FNs and FPs in the last training stage, and using massive unlabeled data for mining the valuable information in the early training stage. We argue the self-training requiring such an adjusting strategy to help stable convergence.

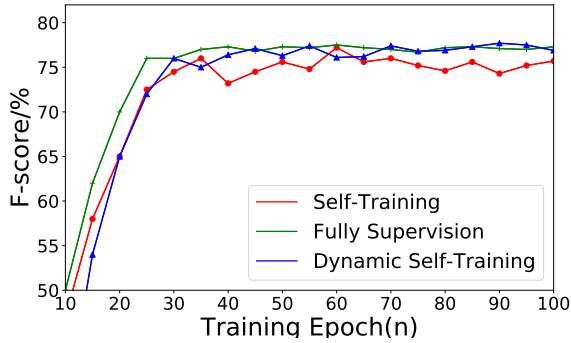


**Figure 8 – Dynamic Mixed Training.** Dynamic Self-Training achieves much stabler convergence compare with common self-training. The EAST [40] is used as the base detector, and the training set of ICDAR2015 is divided into half labeled data and half unlabeled data. ‘Self-Training’ denotes traditional self training without dynamic mixed training.

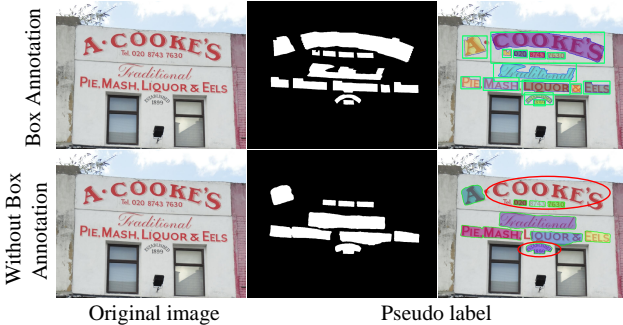


**Figure 9 – The pseudo labels without bounding box annotation contain large amounts of false negatives and false positives, whose performance is not up to using bounding box (i.e., 59.4% v.s. 78.0% for EAST [40] on ICDAR2015).**

Method	Annotation	Evaluation on Total-Text/%		
		Precision	Recall	F-score
PSENet	GT	80.4	76.5	78.4
PSENet	b-GT	46.5	43.6	45.0
PSENet	PL(ST)	80.3	73.5	76.8 (+31.8)
PSENet	PL(Curved ST)	81.7	75.6	78.5 (+33.5)
Evaluation on MSRA-TD500/%				
PSENet	GT	80.6	77.7	79.1
PSENet	b-GT	47.2	36.9	41.4
PSENet	PL(ST)	80.3	77.5	78.9 (+37.5)
EAST	GT	71.8	69.1	70.4
EAST*	PL(ST)	66.6	53.5	59.4
EAST	b-GT	40.5	31.1	35.2
EAST	PL(ST)	71.3	70.2	70.7 (+35.5)

**Table 7 – Box supervision v.s. Strong supervision.** ‘GT’, ‘b-GT’, ‘PL(ST)’, ‘PL(Curved ST)’ denote the ‘Ground Truth’, ‘Bounding box annotation’, ‘Pseudo label generated by BBS with SyntheText’, ‘Pseudo label generated by BBS with Curved SyntheText’, respectively. \* denotes ‘Pseudo label generated by the detector without bounding box annotation’. In blue are the gaps of at least (+31.8) point.

Method	Ratio	Evaluation on ICDAR2015/%		
		Precision	Recall	F-score
Baseline	10%	59.2	59.3	59.2
Baseline+DST	10%	73.7	69.3	71.7 (+10.1)
Baseline	30%	71.8	69.3	70.5
Baseline+DST	30%	76.6	76.0	76.3 (+5.5)
Baseline	50%	76.6	73.6	75.1
Baseline+DST	50%	79.8	76.8	78.3 (+3.2)
Baseline	70%	77.4	76.4	76.9
Baseline+DST	70%	79.1	77.4	78.2 (+1.3)
Baseline	90%	80.3	78.9	79.6
Baseline+DST	90%	80.6	79.8	80.2 (+0.6)
Baseline	100%	81.6	79.5	80.5

**Table 8 – Labeled data size for DST.** We use PSENet [30] as the base detector. ‘Ratio’ denotes  $\frac{\text{labeled data size}}{\text{total data size}}$ , where the total data size is 1,000 training images for ICDAR2015 [13]. In blue are the gaps of at least (+0.6) point.

### 6.2. Ablation Study

**Box supervision v.s. Strong supervision.** Compare with strong supervision, Bounding Box Supervision (BBS) not only can save significant costs, but also achieves almost the same performance as that of strong supervision. In Tab. 7, we adopt two detectors (i.e., PSENet [30] and EAST [40]) and two datasets (i.e., Total-Text [4] and (MSRA-TD500 [37]) to prove the conclusion. On Total-Text, PSENet using the pseudo label generated by BBS achieve a satisfactory F-score (78.5%), which is almost the same as using the ground truth (78.4%), with 33.5% improvement over that of using the bounding box (45.0.5%). On MSRA-TD500, compared with that using ground truth, EAST and PSENet all achieve the competitive F-scores (70.7% v.s. 70.4% and 78.9% v.s. 79.1%)



**Figure 10** – The visualization of bounding-box annotation, polygon-based ground truth and polygon-based pseudo labels generated by BBS on two datasets: Total-Text [4] and MSRA-TD500[37].

with the pseudo label from BBS, which have great improvements (35.5% and 37.5%, respectively). The competitive performance of BBS proves the practicability efficiency of the pseudo label, Fig. 10 gives some visualization of the pseudo label.

Besides, bounding box annotation as the priori location is necessary for BBS. Fig. 9 gives a visualization comparison between based on bounding box annotation and without the box annotation, the pseudo label without box priori location contains large amounts of false negatives and false positives (the red circle), which causes unsatisfactory performances (*i.e.*, 59.4% *v.s.* 78.0% for EAST [40] on ICDAR2015 [13]), as shown in Tab. 7.

**Labeled data size for DST.** The target of Dynamic Self-Training is using limited labeled data and unlabeled data to train detectors. However, how much labeled data is enough for training a competitive model. Tab. 8 give a correlation between labeled data proportion and performance on ICDAR2015 [13]. F-score is increasing with labeled data proportion increase and achieves a competitive performance (78.3%) with 50% labeled data. Besides, DST brings a significant improvement up to 10.1% while using only 10.0% labeled training set.

## References

- [1] Youngmin Baek, Bado Lee, Dongyoon Han, Sangdoo Yun, and Hwalsuk Lee. Character region awareness for text detection. In *Proceedings of the IEEE Conference on Computer Vision and Pattern Recognition*, pages 9365–9374, 2019.
- [2] Hakan Bilen and Andrea Vedaldi. Weakly supervised deep detection networks. In *Proceedings of the IEEE Conference on Computer Vision and Pattern Recognition*, pages 2846–2854, 2016.
- [3] Gary Bradski and Adrian Kaehler. Learning opencv: Computer vision with the opencv library. ” O’Reilly Media, Inc.”, 2008.
- [4] Chee Kheng Ch’ng and Chee Seng Chan. Total-text: A comprehensive dataset for scene text detection and recognition. In *Proc. Int. Conf. Document Analysis Recogn.*, pages 935–942, 2017.
- [5] Chee Kheng Ch’ng and Chee Seng Chan. Total-text: A comprehensive dataset for scene text detection and recognition. In *2017 14th IAPR International Conference on Document Analysis and Recognition (ICDAR)*, volume 1, pages 935–942. IEEE, 2017.
- [6] Jifeng Dai, Kaiming He, and Jian Sun. Boxesup: Exploiting bounding boxes to supervise convolutional networks for semantic segmentation. In *Proceedings of the IEEE international conference on computer vision*, pages 1635–1643, 2015.
- [7] Dan Deng, Haifeng Liu, Xuelong Li, and Deng Cai. Pixellink: Detecting scene text via instance segmentation. In *Proc. AAAI Conf. Artificial Intell.*, pages 6773–6780, 2018.
- [8] Lijun Ding and Ardesir Goshtasby. On the canny edge detector. *Pattern Recognition*, 34(3):721–725, 2001.
- [9] Ankush Gupta, Andrea Vedaldi, and Andrew Zisserman. Synthetic data for text localisation in natural images. In *Proceedings of the IEEE conference on computer vision and pattern recognition*, pages 2315–2324, 2016.
- [10] Ankush Gupta, Andrea Vedaldi, and Andrew Zisserman. Synthetic data for text localisation in natural images. In *Proc. IEEE Conf. Comp. Vis. Patt. Recogn.*, pages 2315–2324, 2016.
- [11] Kaiming He, Xiangyu Zhang, Shaoqing Ren, and Jian Sun. Deep residual learning for image recognition. In *Proceedings of the IEEE conference on computer vision and pattern recognition*, pages 770–778, 2016.
- [12] Vadim Kantorov, Maxime Oquab, Minsu Cho, and Ivan Laptev. Contextlocnet: Context-aware deep network models

- for weakly supervised localization. In *European Conference on Computer Vision*, pages 350–365. Springer, 2016.
- [13] Dimosthenis Karatzas, Lluís Gomez-Bigorda, Angelos Nicolaou, Suman Ghosh, Andrew Bagdanov, Masakazu Iwamura, Jiri Matas, Lukas Neumann, Vijay Ramaseshan Chandrasekhar, Shijian Lu, et al. Icdar 2015 competition on robust reading. In *Proc. Int. Conf. Document Analysis Recogn.*, pages 1156–1160, 2015.
- [14] Daesik Kim, Gyujeong Lee, Jisoo Jeong, and Nojun Kwak. Tell me what they’re holding: Weakly-supervised object detection with transferable knowledge from human-object interaction. In *AAAI*, pages 11246–11253, 2020.
- [15] Suha Kwak, Minsu Cho, Ivan Laptev, Jean Ponce, and Cordelia Schmid. Unsupervised object discovery and tracking in video collections. In *Proceedings of the IEEE international conference on computer vision*, pages 3173–3181, 2015.
- [16] Minghui Liao, Baoguang Shi, Xiang Bai, Xinggang Wang, and Wenyu Liu. Textboxes: A fast text detector with a single deep neural network. In *Proc. AAAI Conf. Artificial Intell.*, pages 4161–4167, 2017.
- [17] Minghui Liao, Zhen Zhu, Baoguang Shi, Gui-song Xia, and Xiang Bai. Rotation-sensitive regression for oriented scene text detection. In *Proc. IEEE Conf. Comp. Vis. Patt. Recogn.*, pages 5909–5918, 2018.
- [18] Tsung-Yi Lin, Piotr Dollár, Ross Girshick, Kaiming He, Bharath Hariharan, and Serge Belongie. Feature pyramid networks for object detection. In *Proceedings of the IEEE conference on computer vision and pattern recognition*, pages 2117–2125, 2017.
- [19] Jonathan Long, Evan Shelhamer, and Trevor Darrell. Fully convolutional networks for semantic segmentation. In *Proc. IEEE Conf. Comp. Vis. Patt. Recogn.*, pages 3431–3440, 2015.
- [20] Shangbang Long, Yushuo Guan, Bingxuan Wang, Kaigui Bian, and Cong Yao. Rethinking irregular scene text recognition. *arXiv*, pages arXiv–1908, 2019.
- [21] Shangbang Long, Jiaqiang Ruan, Wenjie Zhang, Xin He, Wenhao Wu, and Cong Yao. Textsnake: A flexible representation for detecting text of arbitrary shapes. *Proc. Eur. Conf. Comp. Vis.*, pages 20–36, 2018.
- [22] Pengyuan Lyu, Minghui Liao, Cong Yao, Wenhao Wu, and Xiang Bai. Mask textspotter: An end-to-end trainable neural network for spotting text with arbitrary shapes. In *Proc. Eur. Conf. Comp. Vis.*, pages 67–83, 2018.
- [23] Jianqi Ma, Weiyuan Shao, Hao Ye, Li Wang, Hong Wang, Yingbin Zheng, and Xiangyang Xue. Arbitrary-oriented scene text detection via rotation proposals. *IEEE Trans. Multimedia*, 20(11):3111–3122, 2018.
- [24] Nibal Nayef, Fei Yin, Imen Bizid, Hyunsoo Choi, Yuan Feng, Dimosthenis Karatzas, Zhenbo Luo, Umapada Pal, Christophe Rigaud, Joseph Chazalon, et al. Icdar2017 robust reading challenge on multi-lingual scene text detection and script identification-rrc-mlt. In *2017 14th IAPR International Conference on Document Analysis and Recognition (ICDAR)*, volume 1, pages 1454–1459. IEEE, 2017.
- [25] Ilija Radosavovic, Piotr Dollár, Ross Girshick, Georgia Gkioxari, and Kaiming He. Data distillation: Towards omni-supervised learning. In *Proceedings of the IEEE conference on computer vision and pattern recognition*, pages 4119–4128, 2018.
- [26] Shaoqing Ren, Kaiming He, Ross Girshick, and Jian Sun. Faster r-cnn: Towards real-time object detection with region proposal networks. In *Proc. Advances in Neural Inf. Process. Syst.*, pages 91–99, 2015.
- [27] Baoguang Shi, Xiang Bai, and Serge Belongie. Detecting oriented text in natural images by linking segments. In *Proc. IEEE Conf. Comp. Vis. Patt. Recogn.*, pages 2550–2558, 2017.
- [28] Zhi Tian, Weilin Huang, Tong He, Pan He, and Yu Qiao. Detecting text in natural image with connectionist text proposal network. In *Proc. Eur. Conf. Comp. Vis.*, pages 56–72, 2016.
- [29] Lijun Wang, Huchuan Lu, Yifan Wang, Mengyang Feng, Dong Wang, Baocai Yin, and Xiang Ruan. Learning to detect salient objects with image-level supervision. In *Proceedings of the IEEE Conference on Computer Vision and Pattern Recognition*, pages 136–145, 2017.
- [30] Wenhao Wang, Enze Xie, Xiang Li, Wenbo Hou, Tong Lu, Gang Yu, and Shuai Shao. Shape robust text detection with progressive scale expansion network. In *Proc. IEEE Conf. Comp. Vis. Patt. Recogn.*, pages 9336–9345, 2019.
- [31] Wenhao Wang, Enze Xie, Xiaoge Song, Yuhang Zang, Wenjia Wang, Tong Lu, Gang Yu, and Chunhua Shen. Efficient and accurate arbitrary-shaped text detection with pixel aggregation network. In *Proc. IEEE Int. Conf. Comp. Vis.*, pages 8440–8449, 2019.
- [32] Xiaolong Wang and Abhinav Gupta. Unsupervised learning of visual representations using videos. In *Proceedings of the IEEE international conference on computer vision*, pages 2794–2802, 2015.
- [33] Enze Xie, Yuhang Zang, Shuai Shao, Gang Yu, Cong Yao, and Guangyao Li. Scene text detection with supervised pyramid context network. In *Proc. AAAI Conf. Artificial Intell.*, volume 33, pages 9038–9045, 2019.
- [34] Qizhe Xie, Minh-Thang Luong, Eduard Hovy, and Quoc V Le. Self-training with noisy student improves imagenet classification. In *Proceedings of the IEEE/CVF Conference on Computer Vision and Pattern Recognition*, pages 10687–10698, 2020.
- [35] Yongchao Xu, Yukang Wang, Wei Zhou, Yongpan Wang, Zhibo Yang, and Xiang Bai. Textfield: Learning a deep direction field for irregular scene text detection. *IEEE Transactions on Image Processing*, 28(11):5566–5579, 2019.
- [36] Zhenheng Yang, Dhruv Mahajan, Deepti Ghadiyaram, Ram Nevatia, and Vignesh Ramanathan. Activity driven weakly supervised object detection. In *Proceedings of the IEEE Conference on Computer Vision and Pattern Recognition*, pages 2917–2926, 2019.
- [37] Cong Yao, Xiang Bai, Wenyu Liu, Yi Ma, and Zhuowen Tu. Detecting texts of arbitrary orientations in natural images. In *Proc. IEEE Conf. Comp. Vis. Patt. Recogn.*, pages 1083–1090, 2012.

- [38] Liu Yuliang, Jin Lianwen, Zhang Shuaitao, and Zhang Sheng. Detecting curve text in the wild: New dataset and new solution. *arXiv preprint arXiv:1712.02170*, 2017.
- [39] Zheng Zhang, Chengquan Zhang, Wei Shen, Cong Yao, Wenyu Liu, and Xiang Bai. Multi-oriented text detection with fully convolutional networks. In *Proc. IEEE Conf. Comp. Vis. Patt. Recogn.*, pages 4159–4167, 2016.
- [40] Xinyu Zhou, Cong Yao, He Wen, Yuzhi Wang, Shuchang Zhou, Weiran He, and Jiajun Liang. East: an efficient and accurate scene text detector. In *Proc. IEEE Conf. Comp. Vis. Patt. Recogn.*, pages 5551–5560, 2017.
- [41] Barret Zoph, Golnaz Ghiasi, Tsung-Yi Lin, Yin Cui, Hanxiao Liu, Ekin D Cubuk, and Quoc V Le. Rethinking pre-training and self-training. *arXiv preprint arXiv:2006.06882*, 2020.